Electronic Supplementary Information for Dalton Transactions

Synthetic strategies towards ruthenium-porphyrin conjugates for anticancer activity.

Teresa Gianferrara,[a]* Ioannis Bratsos,[b] Elisabetta Iengo,[b] Barbara Milani,[b] Adrian Oštrić,[b] Cinzia Spagnul,[a] Ennio Zangrando[b] and Enzo Alessio[b]*

[a] Department of Pharmaceutical Sciences, University of Trieste, 34127 Trieste, Italy.

[b] Department of Chemical Sciences, University of Trieste, 34127 Trieste, Italy. E-mail: alessi@units.it

Supplementary Material

Spectral data for selected *meso*-(*p*-nitrophenyl)porphyrins *p*(NO_2)$_n$PP (n = 1-4) and *meso*-(*p*-aminophenyl)porphyrins *p*(NH_2)$_n$PP (n = 1-4).

***p*(NO$_2$)PP**. δ_H ($CDCl_3$): -2.76 (br s, 2H, NH), 7.77 (m, 9H, *p*+*m*Ph), 8.22 (d, J = 3.2 Hz, 6H, oPh), 8.40 (d, J = 8.7 Hz, 2H, *o*NO_2Ph), 8.64 (d, J = 8.6 Hz, 2H, *m*NO_2Ph), 8.75 (d, J = 4.7 Hz, 2H, βH), 8.86 (m, 6H, βH).

***p*(NH$_2$)PP**. δ_H ($CDCl_3$): -2.75 (br, 2H, NH), 4.02 (s, 2H, NH_2Ph), 7.07 (d, 2H, J = 8.3 Hz, *m*NH_2Ph), 7.75 (m, 9H, *m*+*p*Ph), 7.98 (d, 2H, J = 8.3 Hz, *o*NH_2Ph), 8.20 (m, 6H, *o*Ph), 8.84 (m, 6H, βH), 8.96 (d, 2H, βH). UV-Vis λ_{max} ($CHCl_3$)/nm (ε×10^{-3}/dm^3 mol^{-1} cm^{-1}): 419.5 (395), 515 (18.7), 551 (10.6), 589 (6.8), 645.5 (5.8).

***p*(NH$_2$)$_2$*cis*-PP**. δ_H ($CDCl_3$): -2.73 (br, 2H, NH), 4.01 (s, 4H, NH_2Ph), 7.06 (d, 4H, J = 8.3 Hz, *m*NH_2Ph), 7.75 (m, 6H, *m*+*p*Ph), 7.98 (d, 4H, J = 8.3 Hz, *o*NH_2Ph), 8.22 (d, 4H, J = 7.5 Hz, *o*Ph), 8.82 (d, 4H, βH), 8.93 (d, 4H, βH). UV-Vis λ_{max} ($CHCl_3$)/nm (ε×10^{-3}/dm^3 mol^{-1} cm^{-1}): 421.5 (330), 517.5 (15.4), 555 (10.9), 592.5 (6.5) 650 (6.2).

***p*(NH$_2$)$_2$*trans*-PP**. δ_H ($CDCl_3$): -2.74 (br, 2H, NH), 4.03 (s, 4H, NH_2Ph), 7.07 (d, 4H, J = 8.3 Hz, *m*NH_2Ph), 7.75 (m, 6H *m*+*p*Ph), 7.99 (d, 4H, J = 8.3 Hz, *o*NH_2Ph), 8.20 (d, 4H, J = 7.5 Hz, 4H, oPh), 8.82 (d, 4H, J = 4.7 Hz, βH), 8.91 (d, 4H, J = 4.6 Hz, βH). UV-Vis λ_{max} ($CHCl_3$)/nm (ε×10^{-3}/dm^3 mol^{-1} cm^{-1}): 421.0 (336), 517 (15.8), 555 (11.0), 592 (6.1), 650 (5.9).

***p*(NO$_2$)$_3$PP**. δ_H ($CDCl_3$): -2.77 (br s, 2H, NH), 7.80 (m, 3H, *p*+*m*Ph), 8.22 (d, 2H *o*Ph), 8.42 (d, 6H *o*NO_2Ph), 8.68 (d, 6H *m*NO_2Ph), 8.81 (d, 2H βH), 8.92 (m, 6H βH).

***p*(NH$_2$)$_3$PP**. δ_H ($CDCl_3$): -2.73 (br, 2H, NH), 4.01 (s, 6H, NH_2Ph), 7.04 (d, 6H, J = 8.1 Hz, *m*NH_2Ph), 7.73 (m, 3H, *m*+*p*Ph), 7.99 (d, 6H, J = 8.1 Hz, *o*NH_2Ph), 8.21 (dd, 2H, *o*Ph), 8.81 (d, 2H, J = 4.7 Hz, βH), 8.92 (m, 6H, βH). UV-Vis λ_{max} ($CHCl_3$)/nm (ε×10^{-3}/dm^3 mol^{-1} cm^{-1}): 424 (311), 518 (13), 558 (10.6), 554 (5.2), 652 (6.1).

***p*(NH$_2$)$_4$PP**. δ_H ($CDCl_3$): -2.72 (br, 2H, NH), 4.11 (br, 8H, NH_2Ph), 7.05 (d, 8H, J = 8.3 Hz, *m*NH_2Ph), 7.99 (d, 8H, J = 8.3 Hz, *o*NH_2Ph), 8.89 (s, 8H, Hβ). UV-Vis λ_{max} (CH_2Cl_2)/nm: 424, 516, 552, 592, 645.

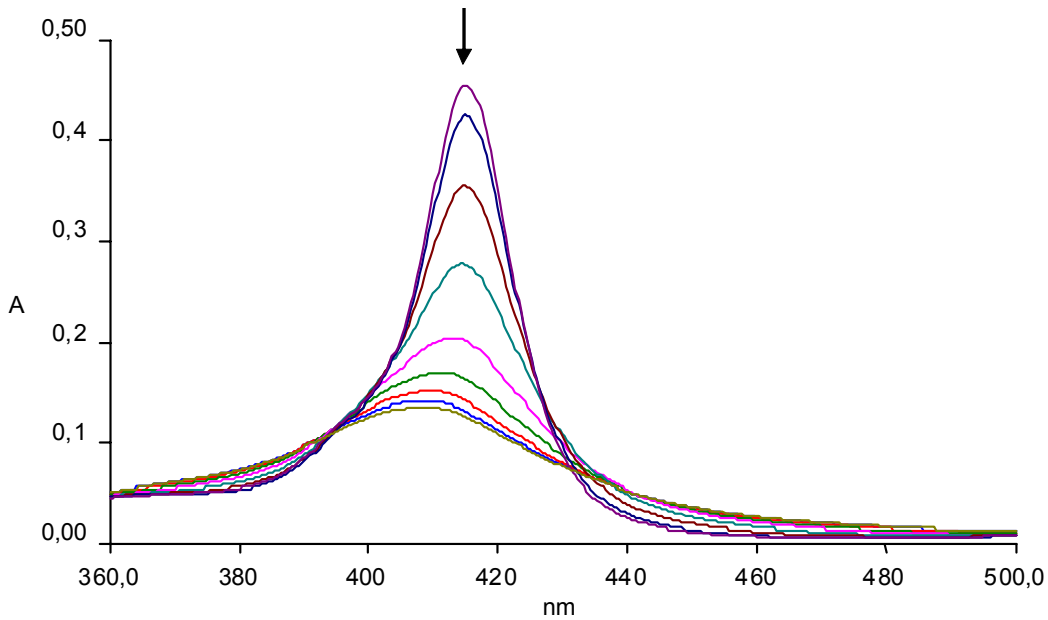

Figure 1S. Time-evolution of the Soret band in the electronic absorption spectrum of $[Na]_4[4'TPyP\{trans\text{-}RuCl_4(dmso\text{-}S)\}_4]$ (**2**) 1.1×10^{-6} M in phosphate buffer 50 mM, pH 7.4, T = 25.0 °C, scan interval = 30 min.

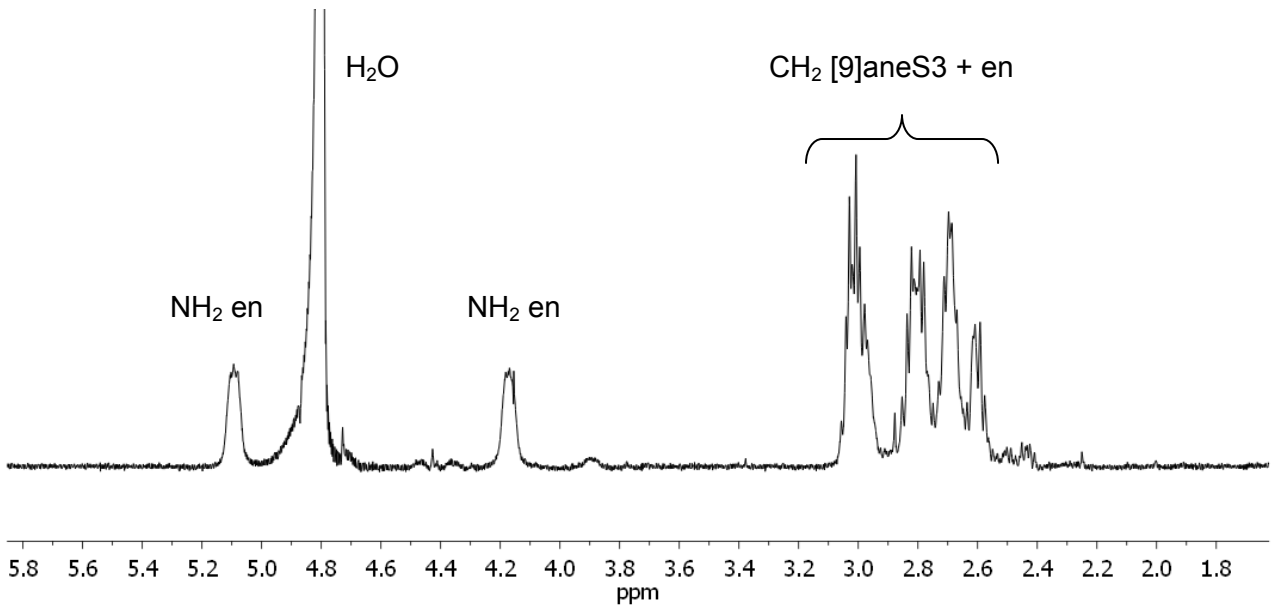

Figure 2S. ^{1}H NMR spectrum (upfield region) of [4'TPyP{Ru([9]aneS3)(en)}$_4$][CF_3SO_3]$_8$ (**3**) in D_2O.

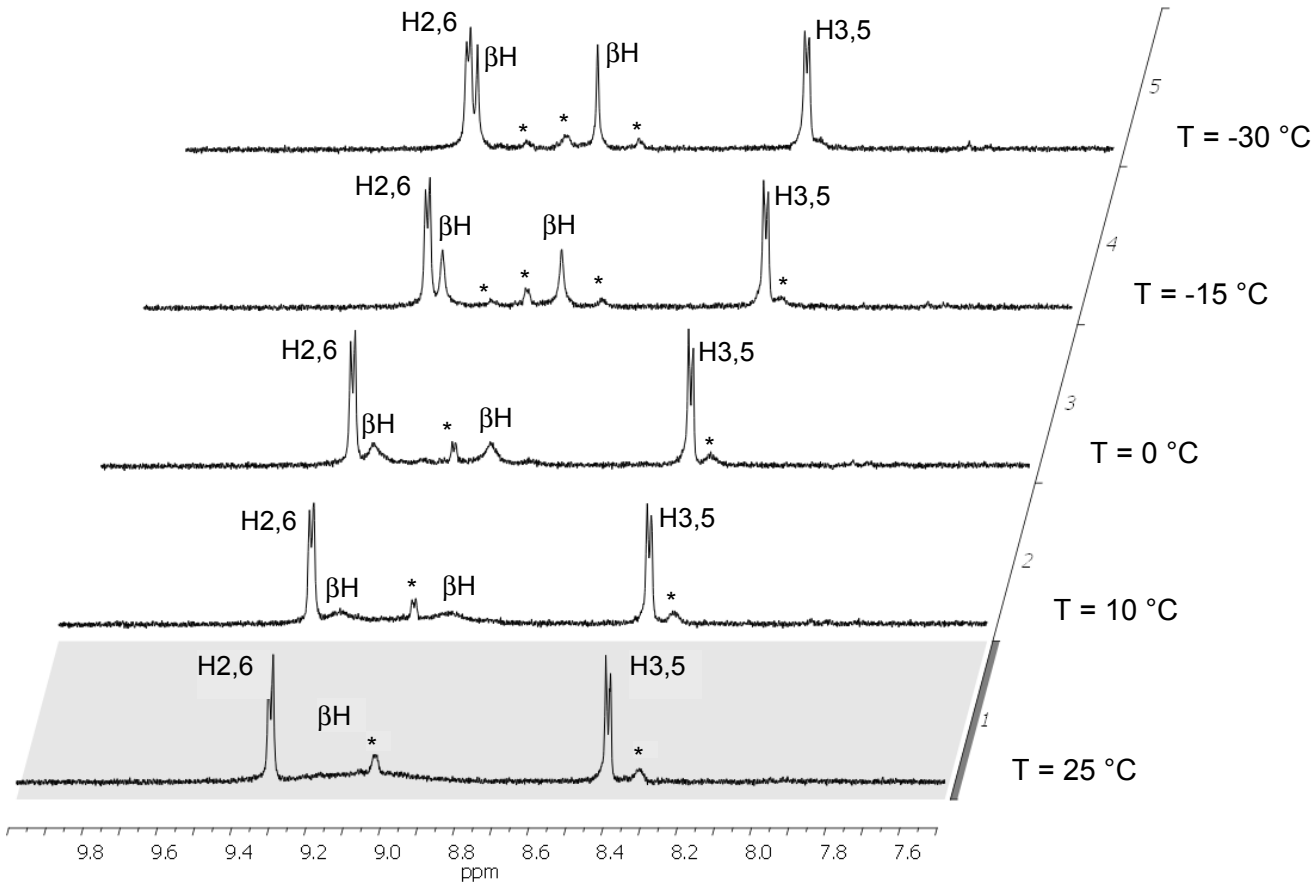

Figure 3S. Temperature dependence of the ^{1}H NMR spectrum (downfield region) of [4'TPyP{Ru([9]aneS3)(en)}$_4$][CF_3SO_3]$_8$ (**3**) in CD_3OD. The asterisk denotes an impurity.

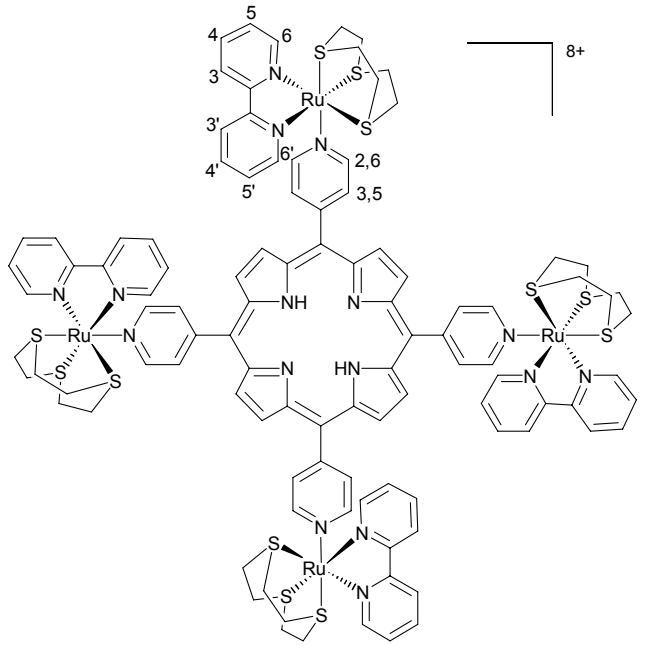

Figure 4S. Schematic drawing and labelling scheme of [4'TPyP{Ru([9]aneS3)(bpy)}$_4$][CF_3SO_3]$_8$ (**4**).

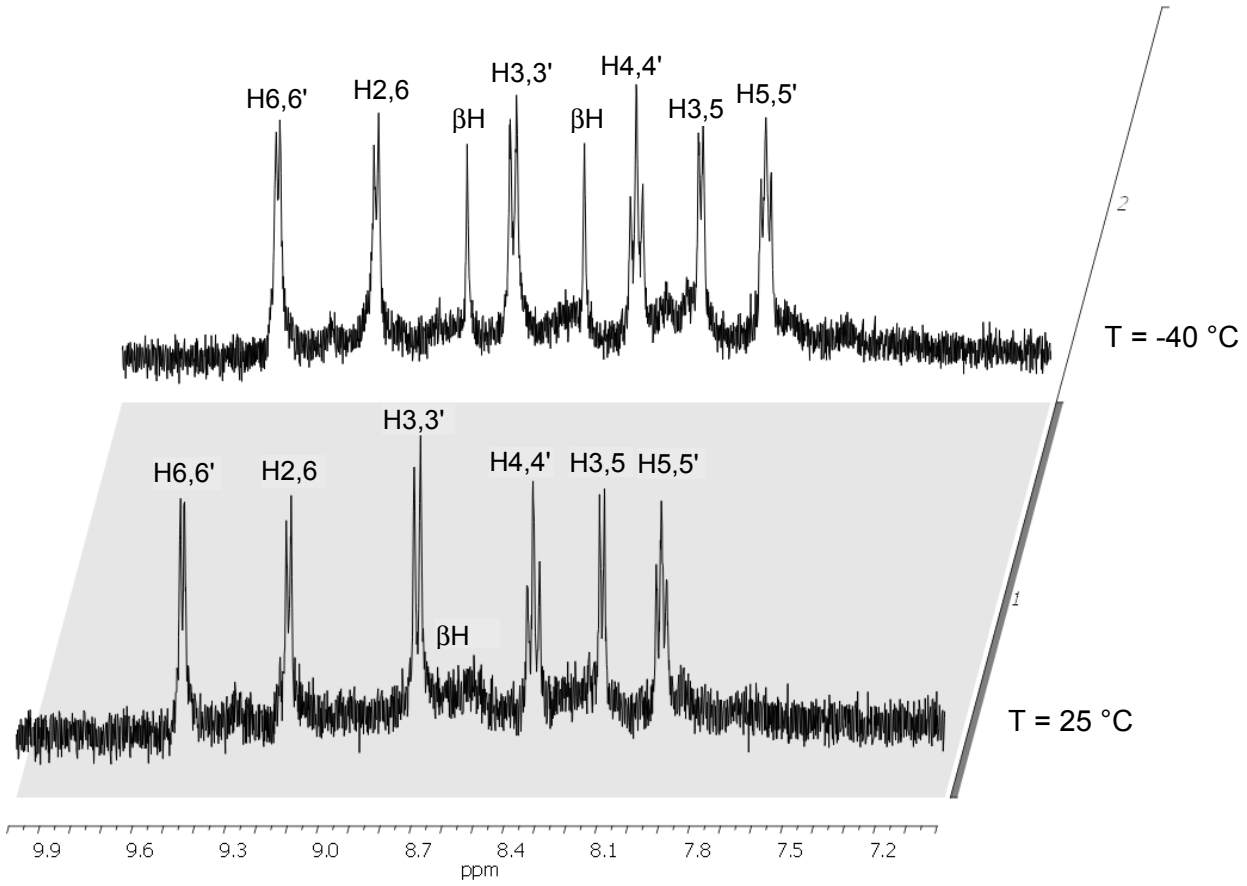

Figure 5S. Temperature dependence of the ^{1}H NMR spectrum (downfield region) of [4'TPyP{Ru([9]aneS3)(bpy)}$_4$][CF_3SO_3]$_8$ (**4**) in CD_3OD/CD_3NO_2 (99:1) solution.

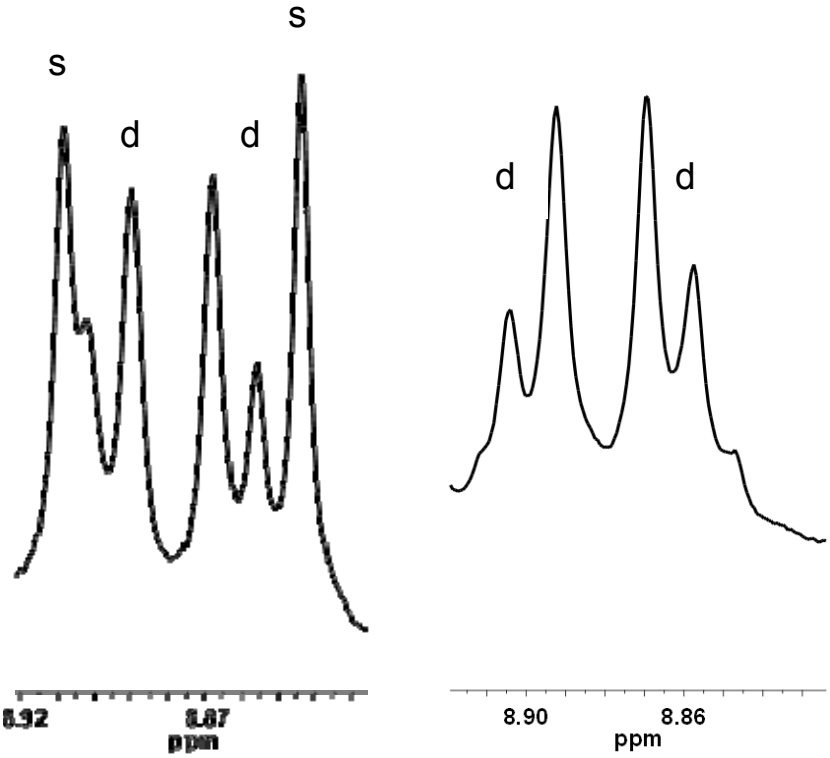

Figure 6S. Region of the βH resonances in the ^{1}H NMR spectra of Bpy$_2$-*cis*PP (left) and Bpy$_2$-*trans*PP (right) in CDCl$_3$.

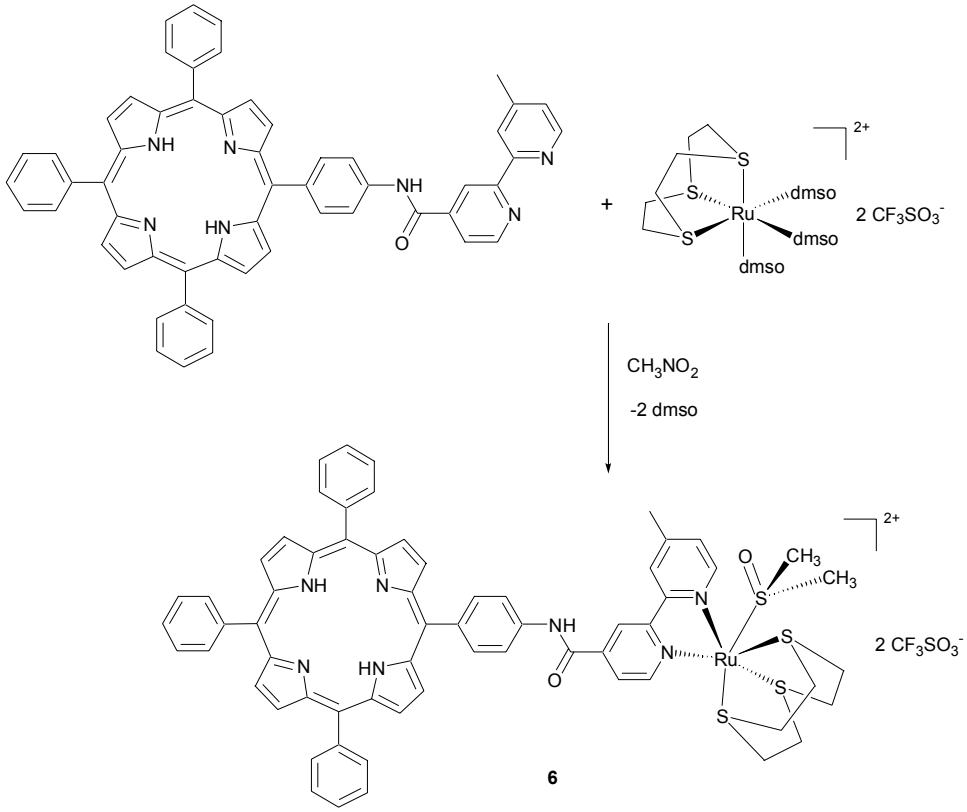

Scheme 1S. Preparation of [Bpy-PP{Ru([9]aneS3)(dmso-S)}][CF$_3$SO$_3$]$_2$ (**6**).

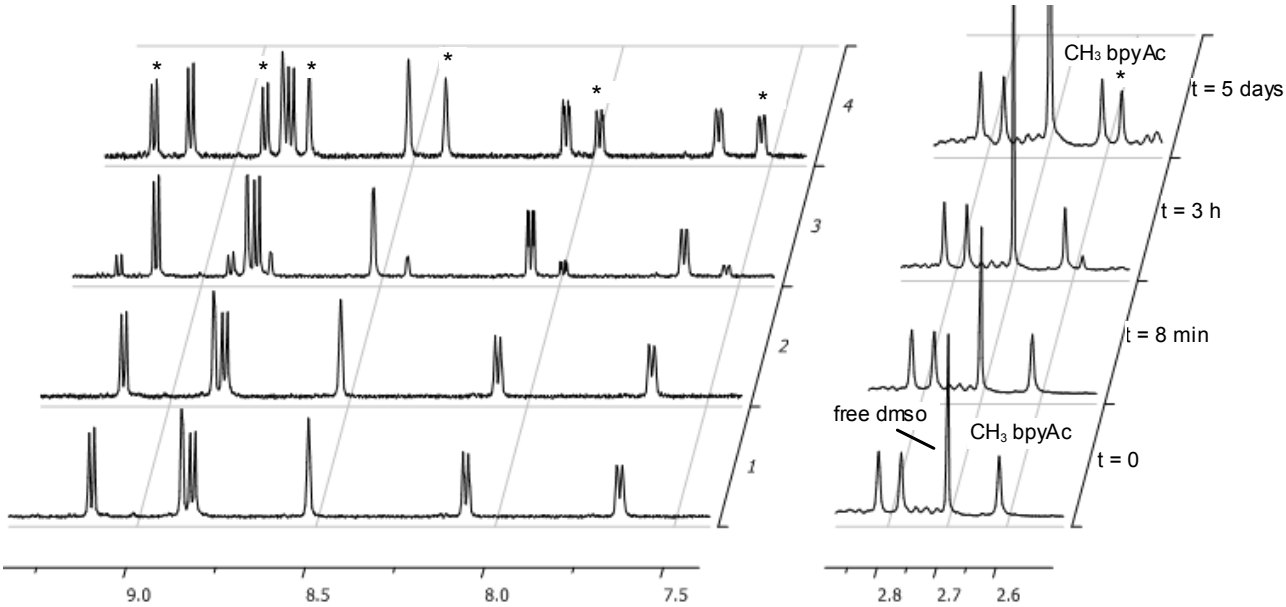

Figure 7S. Time-evolution of the ^{1}H NMR spectrum of [Ru([9]aneS3)(bpyAc)(dmso-S)][CF_3SO_3]$_2$ (**10**) in D_2O. In this case the complex had one molecule of dmso of crystallization (see singlet for free dmso at $\delta = 2.70$ in the initial spectrum). Peaks marked with an asterisk pertain to the aquated species [Ru([9]aneS3)(bpyAc)(H_2O)]$^{2+}$ that slowly grows with time.

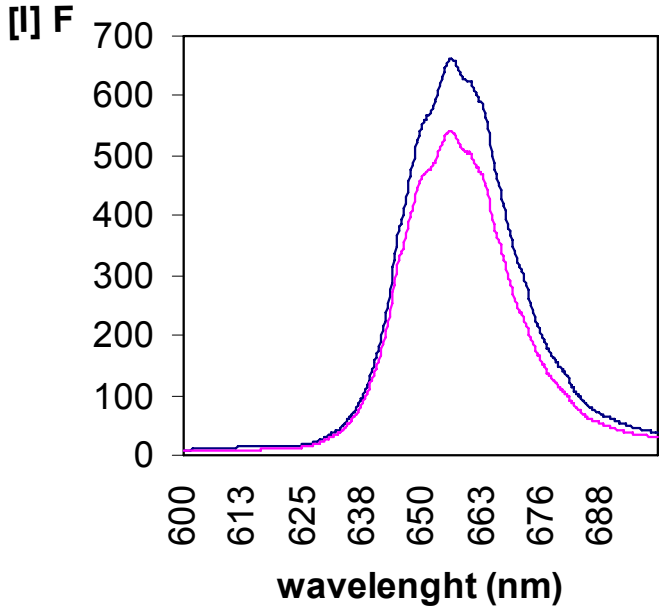

Figure 8S. Fluorescence spectra (λ_{exc} = 425 nm, λ_{em} = 656 nm) of optically matched dmso solutions of Bpy_4-PP (black) and [{Bpy_4-PP}{Ru([9]aneS3)(dmso-S)}$_4$][CF_3SO_3]$_8$ (**9**) (purple).

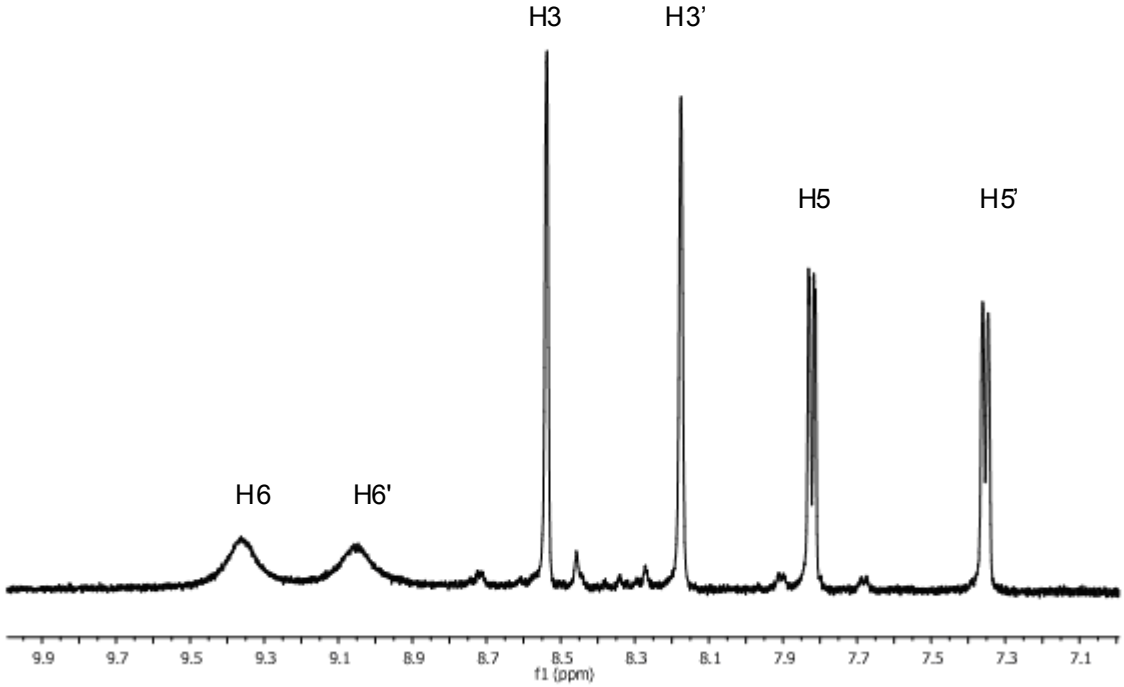

Figure 9S. Aromatic region of the ^{1}H NMR spectrum of [Ru([12]aneS4)(bpyAc)][CF_3SO_3]$_2$ (**12**) in D_2O.

Table 1S. Selected coordination bond lengths (Å) and angles (°) for compound **10**.

Ru–N(1)	2.112(3)	Ru–S(2)	2.341(1)
Ru–N(2)	2.112(3)	Ru–S(3)	2.361(1)
Ru–S(1)	2.334(1)	Ru–S(4)	2.331(1)
N(1)–Ru–N(2)	77.82(13)	N(2)–Ru–S(4)	93.14(9)
N(1)–Ru–S(1)	97.72(10)	S(1)–Ru–S(2)	86.77(4)
N(1)–Ru–S(2)	173.96(10)	S(1)–Ru–S(3)	88.14(5)
N(1)–Ru–S(3)	88.32(9)	S(1)–Ru–S(4)	89.55(4)
N(1)–Ru–S(4)	92.74(9)	S(2)–Ru–S(3)	87.79(4)
N(2)–Ru–S(1)	174.89(9)	S(2)–Ru–S(4)	91.32(4)
N(2)–Ru–S(2)	97.50(10)	S(3)–Ru–S(4)	177.57(4)
N(2)–Ru–S(3)	89.22(9)		